Wasit Journal of Engineering Sciences

Journal homepage: https://ejuow.uowasit.edu.iq

Performance Improvement of Multi-band MIMO Antennas for 5G Applications

Ali F. Hassoon[1*], Radhi Sehen Issa[1*]

Affiliations
[1]Electrical Engineering Department, College of Engineering, Mustansiriyah University, Baghdad, Iraq.

Correspondence
Radhi Sehen Issa,
radhi.sahan@uomustansiriyah.edu.iq

Received
12-October-2024
Revised
10-November-2024
Accepted
20-November-2024

Doi:https://doi.org/10.31185/ejuow.Vol12.Iss4.605

Abstract

This paper provides a good comprehensive argument in favor of the design of 5G and beyond upcoming wireless technology four element Three major frequency band MIMO antenna. The antenna presented in this thesis is built using FR-4 material, is 38 x 38 x 1.67 mm3 in size, and can operate in the UWB, Ku band, and a portion of Ka-band and lower millimeter band. The proposed technique was evaluated utilizing a 4×4 MIMO antenna structure which resonates at three bands. Dimensions of the array are 0.4 × 0.4 × 0.039λ_g^3. The responses of the proposed antenna system to tested features are compatible to broadband frequency ranges. The first band covers frequencies from 3.14 GHz to 9.14 GHz (6 GHz bandwidth) with the following characteristics: 97.A total efficiency of 73%, 7% bandwidth, 78% maximum radiation efficiency. This PMID design achieves a 2.27 dB peak gain, 10 dB average diversity gain (DG), and fails to exceed 0.085 the envelope correlation coefficient (ECC). Additionally, this antenna has more than 24 dB isolation boundary between radiating elements.

This antenna realizes 58% bandwidth, with the operation range from 9.2 GHz to 16.7 GHz (7.5 GHz), but maintaining 88.8% of maximum radiation efficiency, and 82.7% of total efficiency at second band. On average, ~10 dB DG, a peak gain of 5.4 dB, and an ECC beneath 0.018. Also, more than 18 dB minimum decoupling between the adjacent elements. At the third frequency band of 20.15 GHz to 31.31 GHz = 11 GHz bandwidth, corresponding to a 43.4% bandwidth, the proposed structure shows 11 GHz bandwidth. A maximum radiation efficiency of 86.3% (total efficiency of 83.5%) is achieved, and a peak gain of 7.4 dB is achieved. The ECC (<0.005) and average DG (10 dB) are typical for the average DG. The radiating elements are separated by more than 13 dB isolation gap.

Keywords: MIMO, 5G, wireless technology.

1. INTRODUCTION

Wireless communication values highly the versatility and performance of MIMO antennas. With this approach, the RF link and channel capacity are improved [1 - 3]. A system's performance can be enhanced by using certain techniques such as beam forming and diversity, according to the work in [4]. Careful design and suitable performance optimization, announced in [5], enable the researcher to improve the communication system capabilities. Finally, in [6] work is concluded that a MIMO antenna system can provide more generality and sophistication to communication links. According to [7], it is positive to smartly engage each antenna element into the MIMO antenna structure and improve the coverage and range of the antenna system. One of the MIMO array benefits is its beam-forming capability demonstrated in [8]. This beam forms the technique (as described in [8, 9] improves signal quality, and reduces interference dramatically by focusing the transmitted energy to a point directed. Shaping and guiding the signal data stream towards the projected goal or MIMO recipient, [10-13] helps maximize the efficiency of the communication links (transmission and reception). find, by exploring the use of the well-

structured four-element MIMO antenna with λ/4 dual band slots, that high array element decoupling enables performance improvement and interference reduction.

The input impedance at the slot of a λ/2 slot is capacitive-inductive mixed, while the impedance at the slot of a λ/4 slot is purely reactive. The relationship between impedance and bandwidth is crucial in dual-band system design. Proper slot width and distance between the slot and patch edge are essential for impedance matching and optimizing the bandwidth [14].

Mutual coupling affects the performance of a four-port MIMO antenna system. It can cause power loss, interference, and reduced DG. A compact four-port MIMO antenna minimizes mutual coupling and interference from nearby human limbs. Increasing the distance between antennas or using a high permittivity substrate can reduce mutual coupling. Decoupling structures and dielectric materials can mitigate mutual coupling but may require re-simulation [15-18].

The paper [19] describes a MIMO antenna with four ports that have a rectangular shape. Despite its small size of 39 x 39 mm2, the antenna can operate within three frequency bands: 3.25–3.75 GHz, 5.08–5.90 GHz, and 7.06–7.95 GHz. Furthermore, the customized antenna design exhibits a gain oscillating from 1.4 to 4.6 dBi, which leads to amplifying signal strength efficiently. Notably, mitigating undesirable mutual coupling effects by the implementation of a 4-staircase-shaped decoupling technique causes a significant 22 dB isolation between antenna elements. Moreover, the total active reflection coefficient (TARC) remains more than 10 dB, further study reveals this antenna's capability to maximize transmission efficiency and minimize signal reflections. The fabrication process has escalated challenges caused by the structure complexity and the decoupling mechanism used in antenna design.

The 4-port, 3 x 3 Electromagnetic Band Gap (EBG), UWB-MIMO antenna array designed in [20] has the following characteristics: 60 x 60 x 1.6 mm³ structure dimensions, (3 - 16.2) GHz frequency range notched at 4.6 GHz due to the inherent characteristics of the EBG structure. The design realizes a 17.5 dB isolation level. Surface wave propagation suppresses and minimizes mutual coupling due to the use of EBG array arrangement.

The author of [21] presents a comprehensive analysis of a 4-element MIMO antenna with SRR, 136 x 136 mm2. It offers a 2.2-6.28 GHz operating bandwidth, including the following significant bands (LTE, Bluetooth, WLAN, WiMAX, and ISM). However, the design presents a maximum gain of 4 dBi and 14 dB port isolation. This design's efficiency is reduced due to its bulky size and minor port isolation. Another research [22], presents a compact MIMO antenna system with 4-elements for wireless communication applications. It achieves broadband, high isolation, and excellent performance regarding several significant metrics. The design is confirmed for LTE, WLAN, and 5G (sub-6 GHz) range. It has a 4-element formation, a fractional broadband of 52.42%, and top of 27 dB isolation between antenna elements. This MIMO antenna reveals high DG, and MEG, low ECC, as well as low TARC, suitable isolation between antenna ports, and channel capacity loss (CCL).

The study in [29] presents a 5G (sub-6 GHz) MIMO antenna compatible with LTE applications. The core radiator is an I-shaped monopole that resonates at the range of 1.46 GHz to 2.27 GHz feeding from a tapered microstrip line. A modified rectangular stub improves isolation, resulting in low antenna element correlation, high signal reliability, efficient power transmission and reception, minimal interference, and high data throughput [30-40]. This system is suitable for 5G and LTE applications.

The useful information obtained from the literature review is as follows:

- MIMO antennas aid in improving the data rate without requiring extra bandwidth.
- It is a challenge to achieve high performance, high port isolation, and compact size without the need for additional structure in the design.

The suggested design demonstrates scientific innovation through its simplicity and impressive results. It adopts a straightforward structure without incorporating intricate methods or additional components like metamaterials or metallic vias to achieve decoupling, bandwidth, and gain enhancement. This research introduces a concise four-port MIMO antenna that operates between the frequency range of 3–32 GHz. Its design includes a grounded connection and a straightforward decoupling technique. The suggested 4x4 three-band MIMO antenna presents an exciting opportunity for the progression of wireless technology. With its remarkable bandwidths and reduced mutual coupling, it has the potential to deliver exceptional performance for future wireless applications.

The notable key-points of the suggested work can be emphasized in the following manner:

1- The proposed design features symmetrical elliptical-shaped patches that have been integrated above the substrate.

2- In order to improve the isolation and impedance bandwidth of the MIMO elements, a modified partial ground with a rectangular slot (with one side missing) has been utilized. This enhancement enables a wider range of frequencies with better impedance matching. Additionally, decoupling ground-based slots has been implemented to greatly reduce coupling.
3- The antenna design is notable for its compactness, both in terms of its electrical and physical dimensions.
4- Exceptional performance is achieved throughout the entire operating band.
5- A suitable technique has been implemented to decouple the antenna elements and ensure a high level of isolation across the operating band.

The remaining portion of the article is organized in the following manner: Section 2 examines the proposed antenna design. Section 3 focuses on the design layout and assessment. Section 4 deliberates on the simulated findings. Section 5 provides the concluding remarks for the paper.

2. ANTENNA'S UNIT CELL DESIGN

The proposed antenna utilizes a patch antenna's radiating element with slots, aiming to achieve superior functionality. The initial design process involves creating a single elliptical microstrip patch antenna, measuring 12.3 mm × 10.2 mm, integrating a feeding element sized at 2.8 mm × 4.8 mm. As depicted in Figure 1, this specific antenna is produced on an FR-4 substrate. The FR-4 substrate is well-known for its loss tangent value of 0.025 and a dielectric constant of 4.3.

The bandwidth of the patch antenna is directly influenced by the radius of the semi-circle. In this case, the radius is determined by applying equations (1), (2), and (3) [1]. These equations take into account the height of the substrate (h), the substrate's dielectric constant (εr), the resonant frequency (fr), and the speed of light (C), which is 3 × 108 m/s.

$$R = \frac{K}{\sqrt{1+\frac{1}{\alpha\varepsilon_r}(ln(\alpha))+1.7726}} \quad (1)$$

$$K = \frac{8.791*10^9}{f_r} \quad (2)$$

$$\alpha = \frac{\pi K}{2h} \quad (3)$$

(a) (b)

Fig. 1 Unit cell of the proposed MIMO antenna with (50 Ω impedance) (a) patch side, (b) ground side.

Table 1. presents the recommended dimensions for optimizing antenna elements, measured in millimeters.

Parameter	dimension (mm)	Parameter	dimension (mm)
Ls	19	**Ws**	23

Lf	4.71	**Wf**	2.91
R1	5.53	**R2**	2.15
R3	2.15	**R4**	2.15
R5	2.2		
Lg	8	**Wg**	8
Lgs	9	**gse1**	1.9
Rg	6		

3. OPTIMIZING IMPEDANCE MATCHING AND RADIATION EFFICIENCY

Analyzing the modified ground plane presented in Figure 1b, when R1 is set to 6 mm and R2 is set to 5mm, the input impedance reaches its pinnacle and leads to an equal distribution of current. The objective is to achieve optimal impedance matching and radiation efficiency while keeping the design compact, to separate components operating in three frequency bands. Experts advise aiming for impedance matching around 100 ohms for λ/4 to λ/8 slots and feeding lines, and around 200 ohms for λ/2 slots. Adjustments are made to ensure a perfect match at the resonant frequency by using a 50-ohm microstrip line to transmit voltage. In the case of λ/4 slots, the resonant frequency deliberately shifts closer to the operating frequency to improve impedance matching. It is crucial for each radiating element to operate within its efficiency bandwidth in order to achieve the optimal impedance matching and radiation efficiency. The most essential information regarding the optimal match can be obtained from the highest real part of the input impedance, which occurs at R1 = 6mm and R2 = 5mm. This guarantees an even distribution of current along the radiation patch. The primary objective of the design is to enhance impedance matching, radiation efficiency, layout compactness, and isolation between radiation elements. Impedance matching is based on existing knowledge and literature. Through simulation, the strategic placement of slot cuts on the radiating patch effectively decreases mutual coupling in the MIMO antenna. Additionally, specific dimensions for decoupling slots help minimize mutual coupling. The isolating element, additional capacitance from slots, and capacitance achieved through the dielectric substrate all work together to ensure high isolation and minimal mutual coupling. The desired outcome is an efficiency of 90% and a gain of 5.5dB.

Notably, the designed antenna has the remarkable capability to cover the UWB, Ku-band, and a section of the Ka-band and lower millimeter band, as illustrated in Figure 2.

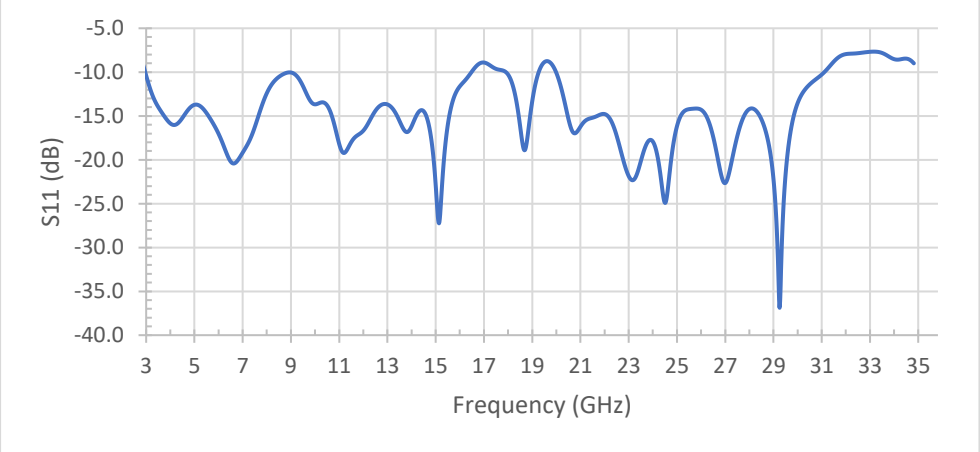

Fig. 2 illustrates the reflection coefficient, (S11), for an individual component in relation to the frequency resonant bands.

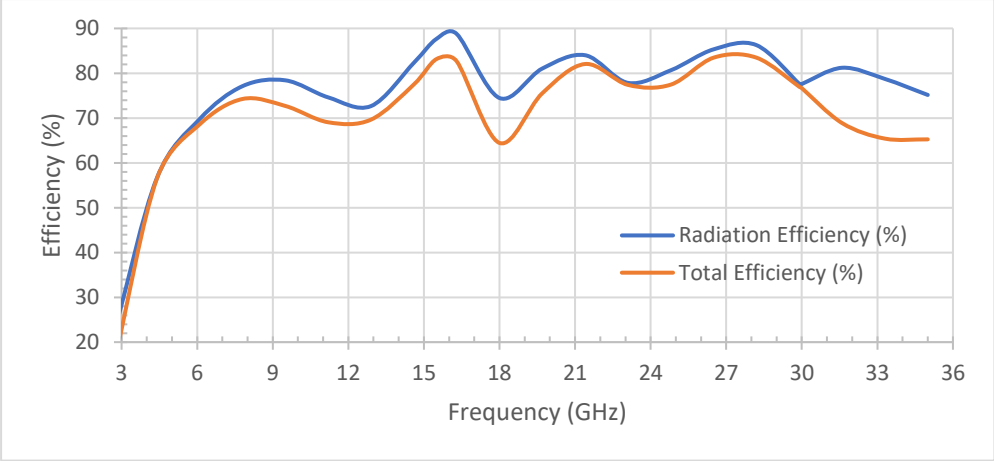

Fig. 3 shows the antenna's operational efficiency based on the frequency

As per the data for individual elements shown in Figure 3, the maximum radiation efficiency and total efficiency of the antenna are established at 89% and 83%, respectively. Conversely, the findings from the simulations illustrated in Figure 4 indicate that the suggested antenna exhibits worthy performance with respect to gain-bandwidth operation with a maximum gain is 9.2 dB.

- **Semi-Circular Patch:** The antenna element utilizes a semi-circular patch shape, which contributes to its broadband characteristics. The circular geometry allows for a wider range of resonant frequencies compared to traditional rectangular patches.
- **Slots and Openings:** The presence of slots and openings within the patch structure further influences the current distribution and impedance characteristics, contributing to the broadband behavior and potentially improving isolation between elements in a MIMO configuration.
- **Microstrip Feed:** The antenna is fed using a microstrip line, a common and efficient method for feeding patch antennas.
- **Ground Plane with Decoupling Structure:** The back side of the antenna (Figure 1b) showcases a ground plane with a decoupling structure consisting of meandered lines between the feed points. This is likely implemented to reduce mutual coupling between the antenna elements in a MIMO setup.

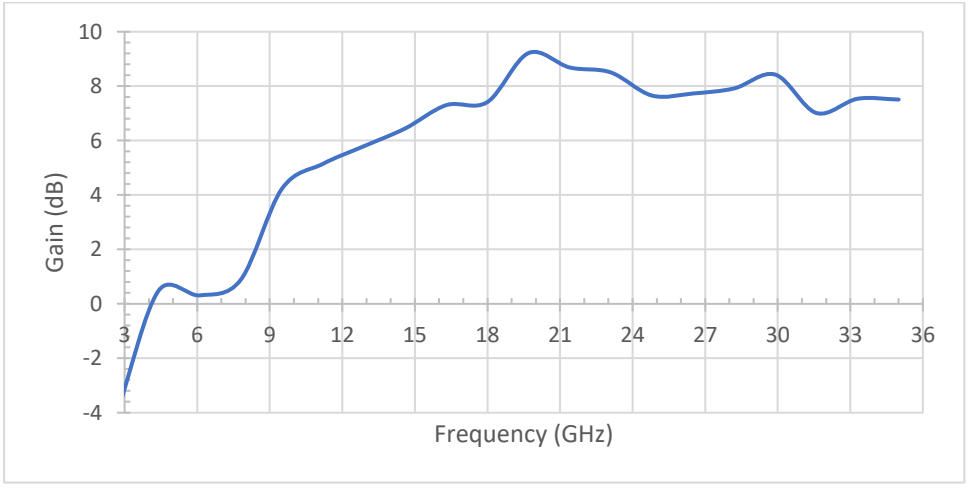

Fig. 4 Shows the simulated Gain of the proposed antenna.

4. MIMO ANTENNA DESIGN ARRANGEMENT

The proposed antenna's design is presented in Figure 5. It has been fabricated on a FR4 substrate with dimensions of 40 x 40 mm^2. The substrate is integrated with four elliptical patch antennas, forming the MIMO antenna configuration. The antenna element spacing is set to 13.14 mm, which correspond to (λ/3, 2λ/3, and λ) where λ is the wavelength of the resonant frequencies of the three operating bands (3.144 — 9.144) GHz, (9.17 —16.67) GHz, and (20.15 —31.31) GHz

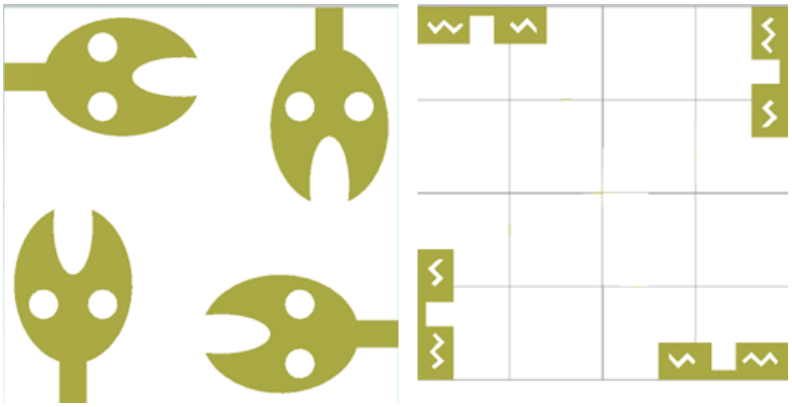

(a) (b)

Fig. 5 Designed Geometry of the MIMO antenna (a) Patch area side, (b) ground area side.

4.1. Enhancing Performance of a Compact Four-Port MIMO Antenna Array

The ports of the radiating elements are oriented orthogonally and spaced apart by 13.14 mm. The diagonal distance between the radiating elements measures 22.23 mm. Figure 5b demonstrates the interconnection of the four ground areas of the MIMO cells through 1 mm thick copper lines. The antennas are arranged in an orthogonal manner to ensure self-decoupling. Additionally, decoupling slots are strategically positioned on both sides of the ground plane to minimize mutual coupling between the ports. A 1 mm thin copper line is employed to establish connections between the ground plane of each radiating element, effectively reducing surface wave propagations. This technique came in handy for minimizing unwanted mutual coupling between the radiating elements, preventing potential damage to the cable ends, solder contact points, connectors, and antennas caused by induced voltage standing waves.

The developed compensation methods for separating components in MIMO systems efficiently decrease the mutual coupling between adjacent unit cells, enabling a more condensed configuration of antennas. Consequently, the size of the MIMO system is moderated. This antenna, possessing both a compact design and superior capabilities, is capable of functioning across numerous frequency bands including 3G, 4G, 5G, and beyond.

5. RESULTS AND PERFORMANCE EVALUATION

The results depicted in Figure 10 illustrate the bandwidth ranges of the antenna. These ranges show improved isolation and broader frequency coverage, spanning from (3.4 to 10.6) GHz, (11.7 to 18.8) GHz, and (19.5 to 31.3) GHz at each port servicing the UWB, Ku-band, and a portion of the Ka-band and lower 5G millimeter band. The reflection coefficient at Ports 1, 2, 3, and 4 is also shown. Figure 8 demonstrates that the antenna elements are perpendicular to each other. Figure 14 displays the surface current at 5 GHz, 13 GHz, and 28 GHz. Despite the isolation between the ports being less than − 12 dB, Figure 15 portrays the isolation between the ports. To ensure optimal results, the transceiver antennas were even swapped to enable the determination of Isolation coefficients (S12, S21, S13, ..., S42, and S43) for the four antenna MIMO combination. In closing, the customize operation conditions, was presented to evaluate the performance of the MIMO antenna and analyze the attained results. The

S-parameter provides a wide-ranging approach for evaluating antenna performance. By considering various factors, this design has wide applicability in several applications.

5.1. Evaluation of Envelope Correlation Coefficient

The ECC is a proper factor used to evaluate the correlation between two complex signals. A value of 1 indicates a perfect correlation between the signals, while a value of 0 indicates no correlation. In the context of MIMO antenna arrays in wireless communication systems, it is imperative to evaluate the ECC to understand the spatial diversity benefits that can be achieved by utilizing multiple antennas. Assessing the ECC values for the three antenna bands is crucial for determining system performance. The ECC values range from 0 to 0.08, where values below 0.05 indicate a satisfactory level of DG. The ECC calculation is performed for all bands. The use of MIMO antennas leads to advantages resulting from spatial diversity [59][60][58].

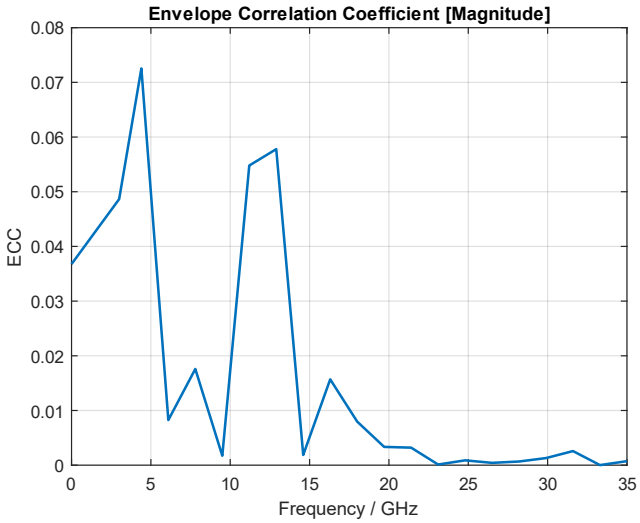

Fig. 6 Shows the proposed design's ECC.

5.2 Evaluation of Diversity Gain

By maintaining a GD of 10 dB, a reduction in input power will have minimal effects on the normal transmission. Figure 7 offers a visual depiction of the modeled DG, which was attained using CST Microwave Studio for simulation. The diagram distinctly illustrates that the mean simulated DG of the suggested array is 9.8, encompassing the entire frequency range of significance. This value closely approaches the desired standard of 10 dB.

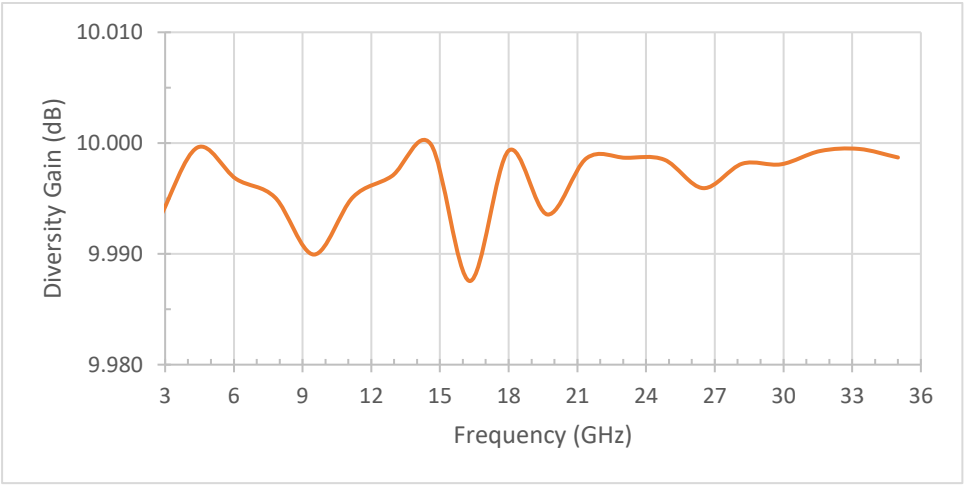

Fig. 7 Shows the proposed design's DG.

5.3 Time Domain Analysis of the Proposed MIMO Antenna

The group delay is an important aspect to consider when studying the time domain. It helps us understand how different frequency components in a signal are delayed as they pass through a system. In Figure 8, you can see a visual representation of the group delay for the recommended MIMO antenna. It shows the delay between port #1 and the other ports across the frequency range of 3 GHz to 35 GHz. It's worth noting that within the operating frequency range of the antenna (3 GHz to 29.4 GHz), the group delay stays below 2 ns. These group delay values are considered acceptable throughout the entire operating range. Although, a value of 3.63 ns at 29.45 GHz which is still considered satisfactory group delay for the MIMO antenna.

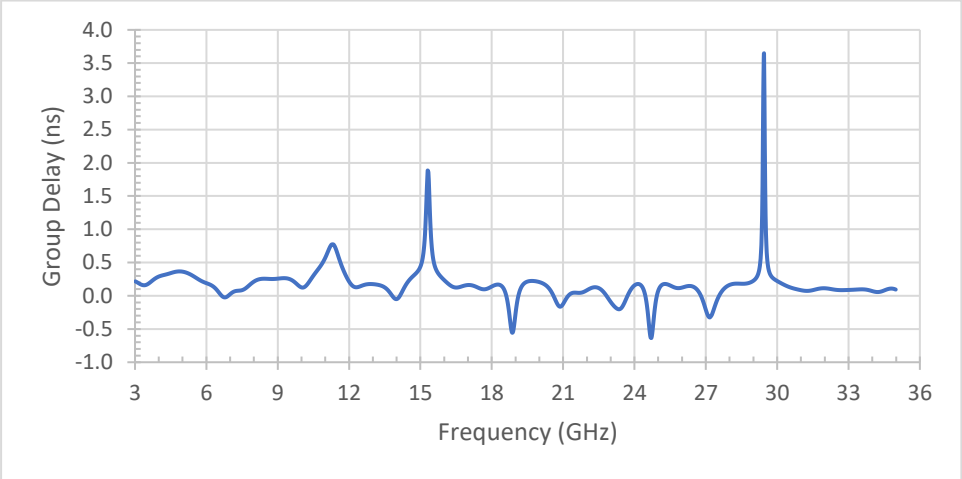

Fig. 8 Shows the proposed antenna array design's Group delay.

6. COMPARISON THE RESULTS WITH THE PREVIOUS STUDIES

In Table 2, a comprehensive examination of the suggested antenna array is presented in contrast to recent research.

Table 2. Comparison the results with the previous studies

Ref. No.	Area (λg^2)/ (mm^2)	BW (MHz)	Peak Gain (dB)	Peak Eff. (%)/ Total Eff. (%)	Max. Isolation (dB)	ECC	Substrate material	Target Application	Technique Used
[23]	(3.52 × 1.76)/ (150 × 75)	200	5.1	82 / NA	16.5	0.01	FR-4	5G	L-shaped strip
[24]	(3.52 × 1.76)/ (150 × 75)	260	1.6	47/ NA	20	0.3	FR-4	5G	M-shaped strip
[25]	(0.45 × 0.45)/ (24 × 22)	2200	NA	NA/ NA	15	0.04	FR-4	5G	NA
[26]	(3.4 × 1.76)/ (145 × 75)	200	4.5	73/ NA	15	0.16	FR-4	5G	L-shaped ground plane deformation
[27]	(5.32 × 5.32)/ (154 × 154)	300	5	-/ NA	40	-	FR-4	NM	Printed Yagi Uda
[28]	(2.63 × 2.63)/ (263 × 263)	1100	7	65/ NA	18	0.159	FR-4	GSM/UMTS/EDGE	Circular Quasi Yagi
[29]	(0.4 × 0.4)/ (80 × 80)	4000	3	84/ NA	15	0.016	FR-4	5G/Sub-6 GHz Wireless application	Self-decoupling technique
[This work]	(40 × 40)/ (14.64 × 12)	6000	2.27	78 / 73	24	0.085	FR-4	5G/UWB/ Ku-band/portion of Ka-band / lower (mmWave) Band Wireless application	Self-decoupling technique
		7500	5.4	88.8 / 82.7	18	0.018			
		11000	7.4	86.3 / 83.5	13	0.005			

The study includes important features such as the array size, the resonant frequencies, maximum gain, the isolation range, the efficiency, the ECC, decoupling method, and the overall performance metrics. The performance analysis followed here indicates that the antenna operates within wide frequency areas, noticing that, the surface area of the antenna was used efficiently, which showed the antenna in a compact and concise profile, this gives it a preference to work in many wireless communication applications. The comparison made here shows that the proposed antenna competes with most, if not all, of the work referred to in terms of radiation efficiency and peak gain as important factors in the superiority of the antenna performance, along with its other capabilities highlighted in the table above.

7. CONCLUSION:

A detailed analysis of the performance of the proposed antenna led to a wide range of resonant behavior around three specific frequency ranges from 3.14 GHz to 31.3 GHz. The antenna has a compelling combination of desirable attributes within these operational bands. For example, to achieve signal integrity, close to 13 dB isolation between adjacent monolithic elements is achieved, leading to low inter-element coupling. In addition, the antenna has an Envelope Correlation Coefficient (ECC) lower than 0.08, strong diversity performance and a robustness against signal decay in multipath environments. The antenna can radiate the power it receives such that a peak efficiency of 88.8% is achieved, and a peak gain of 7.4 dB is obtained, signifying its ability to be directional. Additionally, the antenna has an average Directive Gain (DG) of approximately 10 dB, which is very robust and demonstrates the ability to focus radiated power.

The competitive advantages of the proposed design are demonstrated in a comparative analysis with the existing state of the art antennas for similar applications in terms of these performance metrics. In particular, this antenna differs from previously reported approaches by offering wideband operation, high isolation, low ECC, high efficiency, and appreciable gain. It is these findings that strongly suggest that this antenna is well suited for deployment in demanding fifth generation (5G) and beyond fifth generation (5G) (B5G) communication systems requiring robust performance on a wide operating range. It is demonstrated that the capabilities offered by the antenna make it a promising candidate for integration into next generation wireless devices and infrastructure to provide enhancement in the data rates, increase in reliability and seamless connection in complex communication environments.

REFERENCES:

1. Angelis, C.T.; Chronopoulos, S.K. “System performance of an LTE MIMO downlink in various fading environments”. In Proceedings of the Ambient Media and Systems, Berlin, Germany, 27–28 January 2011; pp. 36–43.
2. Ojaroudiparchin, N.; Shen, M.; Pedersen, G.F. “multi-layer 5G mobile phone antenna for multi-user MIMO communications”. In Proceedings of the 23rd Telecommunications Forum (TELFOR), Belgrade, Serbia, 24–26 November 2015; pp. 559–562.
3. Hassan, N.; Fernando, X. “Massive MIMO Wireless Networks”: An Overview. Electronics 2017, 6, 63.
4. A. Kazmi, M. Zada, S. Islam, and H. Yoo, "Dual-Band MIMO Prototype in the sub-6 GHz Integrated with mm-wave Arrays: Ensuring Beamforming and Safety Measures," IEEE Access, 2024
5. A. A. Aljebory and M. E. Bialkowski, "Tunable dual-band filtering techniques for radar and communication systems," IEEE Transactions on Components, Packaging and Manufacturing Technology, vol. 7, no. 9, pp. 1609-1616, Sept. 2017.
6. J. Zhang, E. Björnson, M. Matthaiou, et al., "Prospective multiple antenna technologies for beyond 5G," IEEE Journal on Selected Areas in Communications, vol. 38, no. 8, pp. 1637-1660, Aug. 2020.
7. P. Tiwari, V. Gahlaut, M. Kaushik, P. Rani, et al., "Advancing 5G connectivity: a comprehensive review of MIMO antennas for 5G applications," International Journal of Antennas and Propagation, vol. 2023, Hindawi, 2023.
8. T. Benedek and J. Vad, "Beamforming based extension of semi-empirical noise modelling for low-speed axial flow fans," Applied Acoustics, 2021.
9. K. S. Mohamed, M. Y. Alias, M. Roslee, et al., "Towards green communication in 5G systems: Survey on beamforming concept," IET Communications, vol. 2021. Wiley Online Library, 2021.
10. J. Zheng, J. Zhang, H. Du, D. Niyato, S. Sun, et al., "Flexible-position MIMO for wireless communications: Fundamentals, challenges, and future directions," IEEE Wireless Communications, 2024.

11. T. Hemalatha and B. Roy, "Ground plane alteration extremely wideband SPAS pair-based MIMO antenna with improved isolation and band notched characteristics," AEU-Int. J. Electron. Commun., vol. xx, no. xx, pp. xx-xx, 2024, Elsevier.
12. LX Wu, YM Pan, SY Zheng, "Millimeter-Wave Wideband Dual-Polarized Aperture-Coupled Magnetoelectric Dipole Antenna Array with High Isolation," in IEEE Transactions on Antennas and Propagation, vol. XX, no. XX, pp. XX-XX, 2024.
13. S.K.P. Patro, R.K. Mishra, and A.K. Panda, "Study of indoor radio coverage performance of dual technology co-existing MIMO antenna platform for low power wireless base station," in Systems and Communications Systems, Springer, 2020.
14. Alnahwi, F. M., et al. "Mutual coupling reduction of a dual-band 2× 1 MIMO antenna using two pairs of λ/4 slots for WLAN/WiMAX applications." (2018): 10-5.
15. M. Srinubabu and N. V. Rajasekhar, "Enhancing Diversity and Isolation Performance for a Four-Port Mimo Antenna in FR-1 5G Frequency Bands," IETE Journal of Research, 2024.
16. A. Khan, Y. He, Z. N. Chen, "A Dual-Band Quad-Port Circularly Polarized MIMO Antenna Based on a Modified Jerusalem-Cross Absorber for Wireless Communication Systems," IEEE Transactions on Antennas and Propagation, 2023.
17. H. Aboelleil, A. A. Ibrahim, et al., "Four-radiator ultra-wideband multiple-input multiple-output antenna with high performance and dual-band rejection features for high-speed communications," Wireless Communication Systems, vol. 2022. Wiley Online Library.
18. D. Gao, Z. X. Cao, S. D. Fu, X. Quan, "A novel slot-array defected ground structure for decoupling microstrip antenna array," in IEEE Transactions on Antennas and Propagation, vol. 68, no. 3, pp. 1612-1621, March 2020.
19. Tang, Z.; Wu, X.; Zhan, J.; Hu, S.; Xi, Z.; Liu, Y. “Compact UWB-MIMO antenna with high isolation and triple band-notched characteristics,” IEEE Access 2019, 7, 19856–19865.
20. Wu,W.; Yuan, B.;Wu, A. Propagation. “A quad-element UWB-MIMO antenna with band-notch and reduced mutual coupling based on EBG structures,”. Int. J. Antennas Propag. 2018, 2018, 1–10.
21. Anitha, R., et al. "A compact quad element slotted ground wideband antenna for MIMO applications." IEEE Transactions on Antennas and Propagation 64.10 (2016): 4550-4553.
22. Singh, Ajit Kumar, Santosh Kumar Mahto, and Rashmi Sinha. "Quad element MIMO antenna for LTE/5G (sub-6 GHz) applications." Journal of Electromagnetic Waves and Applications 36.16 (2022): 2357-2372.
23. Huang, J.; Dong, G.; Cai, J.; Li, H.; Liu, G. A Quad-Port Dual-Band MIMO Antenna Array for 5G Smartphone Applications. Electronics 2021, 10, 542.
24. Li, R.; Mo, Z.; Sun, H.; Sun, X.; Du, G. A Low-Profile and High-isolated MIMO Antenna for 5G Mobile Terminal. Micromachines 2020, 11, 360.
25. Singh, A.K.; Mahto, S.K.; Sinha, R. A compact quad element MIMO antenna for LTE/5G (sub-6 GHz) applications. Frequenz 2022.
26. Liu, Y.; Ren, A.; Liu, H.; Wang, H.; Sim, C. Eight-port MIMO array using characteristic mode theory for 5G smartphone applications. IEEE Access 2019, 7, 45679–45692.
27. Khaleel, H.R.; Al-Rizzo, H.M.; Abbosh, A.; Abushamleh, S. Printed Yagi-Uda array for MIMO systems. In Proceedings of the IEEE Antennas and Propagation Society International Symposium (APSURSI), Orlando, FL, USA, 7–13 July 2013; pp. 1802–1803.
28. Jehangir, S.S.; Sharawi, M.S. A novel dual wideband circular quasi-yagi MIMO antenna system with loop excitation. Microw. Opt. Technol. Lett. 2016, 58, 2769–2774.
29. Salim, H.T.S., et al., A Dumbbell Shape Reconfigurable Intelligent Surface for mm-wave 5G Application. International Journal of Intelligent Engineering & Systems, 2024. 17(6).
30. Sahib, A.Y., et al., Employing topology optimization method to create optimum telecommunication tower design structure. Sustainable Engineering and Innovation, 2024. 6(2): p. 261-274.
31. Al-Rubaye, G.A., and H.T. Hazim, Optimization of capacity in non-Gaussian noise models with and without fading channels for sustainable communication systems. Heritage and Sustainable Development, 2023. 5(2): p. 239-252.
32. Sallomi, A.H. and S.A.J.r. Hashem, A Novel Theoretical Model for Cellular Base Station Radiation Prediction. 2018. 16(17): p. 17.
33. Mohsin, A.I., A.S. Daghal, and A.H. Sallomi, A beamforming study of the linear antenna array using grey wolf optimization algorithm. Indonesian Journal of Electrical Engineering and Computer Science, 2020. 20(3): p. 1538-1546.
34. Kareem, B.A., Z.A.A. Hassain, and A.H. Sallomi. Design of dual high band-notch UWB antenna based on CSRR and parasitic arms. in 2018 18th Mediterranean Microwave Symposium (MMS). 2018. IEEE.
35. Hashim, W.M. and A.H. Sallomi, Broadband Microstrip Antenna for 2G/3G/4G Mobile Base Station Applications. Al-Qadisiyah Journal for Engineering Sciences, 2018. 11(2): p. 165-175.

36. Hassan, S.K., A.H. Sallomi, and M.H. Wali, Design of a Dual-Band Rejection Planar Ultra-Wideband (Uwb) Antenna. Journal of Engineering and Sustainable Development, 2022. 26(4): p. 30-35.
37. Aramice, G.A. and J.Q. Kadhim, Secure Code Generation for Multi-Level Mutual Authentication. TELKOMNIKA (Telecommunication Computing Electronics and Control), 2018. 16(6): p. 2643-2650.
38. Sallomi, A.H., S.K. Hasan, and J.Q. Kadhim, Maximizing Signal Quality for One Dimensional Cells In Mobile Communications. Wasit Journal of Computer and Mathematics Science, 2023. 2(3): p. 86-92.
39. Singh, Ajit Kumar, Santosh Kumar Mahto, and Rashmi Sinha. "A compact quad element MIMO antenna for LTE/5G (sub-6 GHz) applications." Frequenz 77.3-4 (2023): 173-183.